Performance comparison of Protein A affinity-chromatography sorbents for purifying recombinant monoclonal antibodies

Robert L. Fahrner*[1], Duncan H. Whitney†, Martin Vanderlaan‡ and Gregory S. Blank*

*Department of Recovery Sciences, Genentech, Inc., 1 DNA Way, South San Francisco, CA 94080, U.S.A., †POROS Research and Development, PerSeptive Biosystems, 500 Old Connecticut Path, Framingham, MA 01701, U.S.A., and ‡Department of Analytical Chemistry, Genentech, Inc., 1 DNA Way, South San Francisco, CA 94080, U.S.A.

We describe the performance characteristics of five Protein A affinity-chromatography sorbents (Sepharose Fast Flow, Poros 50, Poros LP, Prosep and Streamline) for purifying a recombinant humanized monoclonal antibody from clarified Chinese hamster ovary cell culture fluid. We measured the dynamic capacity at varying flow rates, maximum capacity, pressure drop and production rate. For purified antibody, we measured yield and purity (by SDS/PAGE, the amount of DNA, the amount of host-cell proteins and the amount of Protein A). We found that, whereas all sorbents provided significant and essentially equivalent antibody purification, there were differences in capacity and pressure drop, which affected the production rate and had implications for process applications.

Introduction

Protein A affinity chromatography is a common method for antibody purification. Many commercial Protein A affinity sorbents have been used for antibody purification, including Prosep (controlled-pore glass), Sepharose (cross-linked agarose), Streamline (expanded bed) and Poros (polystyrene/divinylbenzene) [1–9]. Here we directly compare these sorbents for performance characteristics of interest for process chromatography using a recombinant humanized monoclonal antibody in clarified Chinese hamster ovary cell culture fluid. Recombinant humanized monoclonal antibodies are an important class of antibodies because they have therapeutic applications, including the treatment of several types of cancer [10–14]. Protein A affinity chromatography provides a technique for purifying recombinant antibodies because it can selectively bind antibodies in complex solutions, such as harvested cell-culture fluid, allowing impurities to flow through [4,9,15–17].

We directly compared five commercial sorbents, using a recombinant antibody purified from clarified Chinese hamster ovary cell culture fluid. Streamline, an expanded-bed medium, was included and run in a packed bed for comparison purposes. We measured capacity (both dynamic and total), yield, purity (by SDS/PAGE, DNA, Protein A and host-cell proteins), and pressure drop. Dynamic capacity depends on many factors, including the type of Protein A affinity-chromatography medium, ligand destiny, antibody concentration in the load, column temperature and column length, the buffer, conductivity and pH of the load, and the flow rate [3,5–8,18,19]. For each sorbent, we focused on flow rate and column length, which together determine the residence time, because these are easily varied in process applications. Whereas changes in pH, buffer, conductivity or temperature could denature, precipitate or otherwise affect the antibody, changing the flow rate and column length would have little impact on the antibody itself.

We found significant differences between the sorbents in terms of dynamic capacity and pressure drop. The dynamic capacity and the pressure drop contribute to production rate, an important consideration in process chromatography [20–23]. Production rate is the amount of product purified/unit of time per unit of column cross-sectional area or the amount of product purified/unit of time per unit of column volume (CV) [24]. Like dynamic capacity, production rate can depend on many factors, including flow rate and column length [5,22,25,26]. This article focuses on flow rate and column length because they are easily varied to decrease processing time. We derived two simple equations to illustrate how differences in dynamic capacity and pressure drop can affect production rate, and we applied this to an analysis of the sorbents.

Materials and methods

Materials and instruments

In this article, we avoid the use of all-capital nomenclature for commercial sorbents (e.g. Poros instead of POROS) to ensure easy readability. Poros A/M columns, Poros 50 A and Poros A LP media, and BioCAD chromatography instruments were from PerSeptive Biosystems (Framingham, MA, U.S.A.). Prosep A chromatography media were from Bioprocessing (Consett, County Durham, U.K.). Sepharose A Fast Flow and Streamline A were from Pharmacia (Uppsala,

Abbreviation used: CV, column volume.

[1] To whom correspondence should be addressed.

© 1999 Portland Press Ltd

Table 1 Comparative performance values

The pressure drop ($Pa \cdot h^{-1} \cdot cm^{-2}$) was measured on a 10-cm-long column at various flow rates from 100 to 1000 $cm \cdot h^{-1}$, subtracting the system pressure measured on an empty column. The saturation capacity (g of antibody/l of column volume) was measured at 50% breakthrough using the breakthrough curves in Figure 4. The production rate (g of antibody/h per cm^2 of column cross-sectional area or g of antibody/h per l of column volume) is the maximum theoretical production rate given by eqn. (2) and (3) and illustrated in Figure 5 with the constraints described in the text. Values for U_l, L_c, U_e (the flow rate for the elution/equilibration/wash) and Q_d are where the maximum production rate occurs. Values for dynamic capacity (g of antibody/l of column volume), yield (percentage of loaded antibody in the purified pool), host-cell proteins (mg of host-cell proteins/g of antibody), DNA (ng of DNA/mg of antibody) and Protein A (ng of Protein A/mg of antibody) were for runs using a 10-cm-long column and flow rate of 500 $cm \cdot h^{-1}$ (50 $CV \cdot h^{-1}$), loaded to dynamic capacity determined at 1% breakthrough. Values are the means±S.D. of three runs. Load material was clarified Chinese hamster ovary cell culture fluid.

	Poros 50	Poros LP	Prosep	Sepharose	Streamline
Pressure drop ($Pa \cdot h \cdot cm^{-2}$)	22.1	12.4	2.1	7.6	0.7
Saturation capacity (g/l)	25	24	26	38	29
Dynamic capacity (g/l)	17.5±0.1	14.8±0.3	13.0±0.3	10.9±0.3	7.5±0.1
Purified antibody					
Yield (%)	104±1	106±3	103±2	100±2	105±4
Antibody concentration (g/l)	7.1±0.1	6.4±0.4	5.2±0.2	3.8±0.4	3.2±0.1
DNA (ng/mg)	41±3	48±3	40±4	29±2	98±18
Host-cell proteins (mg/g)	2.5±0.2	2.7±0.7	3.7±0.2	4.9±1.2	6.1±2.0
Protein A (ng/mg)	4.6±0.5	7.7±0.4	3.1±0.5	5.7±1.7	6.0±1.7
Areal production rate					
R_{pa} ($g \cdot h^{-1} \cdot cm^{-2}$)	0.17	0.26	0.38	0.20	–
U_l ($cm \cdot h^{-1}$)	690	1020	1490	720	–
L_c (cm)	10.9	11.3	34.3	28.4	–
U_e ($cm \cdot h^{-1}$)	860	1470	1500	750	–
Q_d ($g \cdot l^{-1}$)	16.7	10.5	14.6	20.6	–
Volumetric production rate					
R_{pv} ($g \cdot h^{-1} \cdot l^{-1}$)	17	23	23	13	–
U_l ($cm \cdot h^{-1}$)	700	1000	1000	750	–
L_c (cm)	10.3	11.3	11.1	10.6	–
U_e ($cm \cdot h^{-1}$)	910	1470	1500	740	–
Q_d ($g \cdot l^{-1}$)	16.4	10.6	9.5	5.9	–

Sweden). The DNA Threshold Assay kit was from Molecular Devices (Sunnyvale, CA, U.S.A.). Load material was cell-culture fluid with cells and cell debris removed by tangential flow filtration [27], containing a recombinant humanized monoclonal antibody (IgG1) produced in Chinese hamster ovary cells at a concentration of approx. 0.35 $g \cdot l^{-1}$. This load material was obtained from Genentech (South San Francisco, CA, U.S.A.). Mathematica software was from Wolfram Research (Champaign, IL, U.S.A.). All experiments were performed at 20±5 °C.

Poros 50 and Poros LP

Whereas Poros 50 is a commercially available product, Poros LP is a prototype medium. Poros LP is identical to Poros 50 in terms of bead composition and Protein A ligand density. However, the average particle size of Poros LP is increased in order to increase column permeability by approx. 100% (Table 1), and therefore allow for greater flexibility in process design relative to column length and pressure-drop restrictions. The impact of engineering a population of large interconnected pores on the mass transport of biomolecules to interior binding sites of chromatographic resins has been described [28]. Descriptions have been extended to include the effect of particle size [29] and surface coatings [30] on dynamic capacity. The surface derivatization used to prepare both Poros 50 and Poros LP is intended to yield efficient access of binding sites. The polystyrene/divinylbenzene core is first coated with an amphiphilic co-polymer to render the surface hydrophilic and minimize non-specific binding [31]. Subsequently, a poly(ethylene glycol) chain is bound as an extended flexible spacer arm for the subsequent attachment of recombinant Protein A. The resultant Protein A ligand density is in the range of 5–6 $mg \cdot ml^{-1}$. Poros LP permeability is approx. twice that of Poros 50 (Table 1). The measured nominal particle sizes of the two resins are 55–60 and 45–50 μm, respectively. Since intra-particle flow is a pressure-driven process, it is anticipated that the larger particle size of Poros LP will lead to lower capture efficiency at elevated flow rates compared with Poros 50.

Dynamic capacity

Dynamic capacity was measured at 1% breakthrough using an online assay [32]. The online assay used a 30 mm (length) × 2.1 mm (diameter) Poros A/M (immobilized Protein A, 20 μm particle size) column. Buffer A was 8 mM sodium phosphate/2 mM potassium phosphate/3 mM potassium chloride/137 mM sodium chloride (pH 7.2), and buffer B was 8 mM sodium phosphate/2 mM potassium phosphate/3 mM potassium chloride/137 mM sodium

© 1999 Portland Press Ltd

14708744, 1999, 2, Downloaded from https://iubmb.onlinelibrary.wiley.com/doi/10.1111/j.1470-8744.1999.tb00902.x by Test, Wiley Online Library on [16/10/2023]. See the Terms and Conditions (https://onlinelibrary.wiley.com/terms-and-conditions) on Wiley Online Library for rules of use; OA articles are governed by the applicable Creative Commons License

chloride (pH 2.2). The assay was run on a BioCAD/RPM chromatograph, and used two flow rates, one for run (5.8 ml·min^{-1}) and one for purge (50 ml·min^{-1}). On the BioCAD instrument, purging takes the column out of the flow path, allowing the increased purge flow rate to rapidly fill the flow path with buffer. After purging, the flow rate is decreased and the column is then placed back in line. Detection was at 280 nm. The assay directly sampled the preparative column effluent using an in-line sampling T, with an injection volume of 500 μl. The method was: purge 5 ml of buffer A, run 3 ml of buffer A, inject, run 2.5 ml of buffer A, purge 5 ml of buffer B, run 20 CVs of buffer B. The assay was 2.0 min long. The BioCAD/RPM software automatically integrates the antibody peak and displays the result immediately after the assay is finished. To enable process control (ending loading at 1% breakthrough), the BioCAD/RPM (running the online assay) would give a signal to the BioCAD (running the preparative chromatography) when the appropriate level of breakthrough was reached.

Assays

The antibody concentration in the load material (used to determine yield) was measured by an HPLC assay. The assay used a 0.46 cm (inner diameter) × 10 cm (length) Poros A/M column. The flow rate was 2 ml·min^{-1}, detection was absorbance at 280 nm, and the injection volume was 100 μl. Buffer A was 100 mM sodium phosphate/250 mM sodium chloride (pH 6.3), buffer B was 2% acetic acid/100 mM glycine (pH 3.0), and buffer C was 10% acetic acid. The method was: inject, wash for 2.5 min with 100% buffer A, run a gradient of 100% buffer A to 100% buffer B over 2 min, hold 100% buffer B for 1 min, regenerate with 100% buffer C for 1 min and equilibrate with 100% buffer A for 3 min. The total assay time was 9.5 min.

Yield was determined as the percentage of loaded antibody that eluted in the purified pool. Antibody concentration in the pool was determined by absorbance at 280 nm (with absorbance at 320 nm subtracted to correct for light scattering). DNA was measured using the Molecular Devices DNA Threshold Assay kit. The amount of host-cell proteins (Chinese hamster ovary proteins) was determined by ELISA using goat anti-(host-cell protein) antibodies [33]. SDS/PAGE was performed using a 8–16% Tris/Glycine 1.0 mm × 12 lane gel and the Colloidal Blue staining kit from Novex. Protein A was determined by ELISA.

Preparative chromatography

Preparative chromatography used 1 cm (inner diameter) × 10 cm (length) Omni columns. Three buffers were used. Buffer A was 25 mM Tris/25 mM NaCl/5 mM EDTA (pH 7.1), buffer B was 0.1 M acetic acid (pH 3.5) and buffer C was 2 M guanidine HCl/10 mM Tris (pH 7.5). The column was equilibrated with 5 CVs of buffer A, loaded, washed with 3 CVs of buffer A, eluted with 5 CVs of buffer C and regenerated with 3 CVs of buffer D. Except for experiments to measure dynamic capacity, all columns were equilibrated, loaded, washed, eluted and regenerated at 500 cm/h. The eluted peak was collected by absorbance at 280 nm. Chromatography was run on a BioCAD.

Production rate

Production rate was calculated as the mass of antibody purified in one cycle divided by the time taken to purify the antibody, divided by the column cross-sectional area to make production rate independent of scale. Then:

$$R_{pa} = \frac{V_c Q_d / \{[(V_c Q_d / C_o)/(A_c U_l / 1000)] + [N V_c / (A_c U_e / 1000)]\}}{A_c} \quad (1)$$

where R_{pa} is the areal production rate (g·h^{-1}·cm^{-2}), V_c is the column volume (l), Q_d is the dynamic capacity (g·l^{-1}), C_o is the antibody concentration in the load (g·l^{-1}), N is the number of CVs for the elution/equilibration/wash, A_c is the column cross-sectional area (cm^2), U_l is the flow rate (superficial mobile-phase velocity) for the load (cm·h^{-1}) and U_e is the flow rate (superficial mobile-phase velocity) for the elution/equilibration/wash (cm·h^{-1}). Then $V_c Q_d$ is the mass of antibody purified (g), $V_c Q_d / C_o$ is the volume loaded (l), $N V_c$ is the volume for elution/equilibration/wash (l), and $A_c U_l / 1000$ and $A_c U_e / 1000$ are the volumetric flow rates for the load and the elution/equilibration/wash (l·h^{-1}).

Rearranging terms, eqn. (1) reduces to:

$$R_{pa} = \frac{1}{1000\left(\frac{1}{C_o U_l} + \frac{N}{Q_d U_e}\right)} \quad (2)$$

By dividing by the column length L_c (cm) and converting units, eqn. (2) is transformed to the volumetric production rate R_{pv} (g·h^{-1}·l^{-1}):

$$R_{pv} = \frac{1}{L_c\left(\frac{1}{C_o U_l} + \frac{N}{Q_d U_e}\right)} \quad (3)$$

Actual production rate values were determined graphically from high-resolution contour plots generated in Mathematica.

© 1999 Portland Press Ltd

14708744, 1999, 2, Downloaded from https://iubmb.onlinelibrary.wiley.com/doi/10.1111/j.1470-8744.1999.tb00902.x by Test, Wiley Online Library on [16/10/2023]. See the Terms and Conditions (https://onlinelibrary.wiley.com/terms-and-conditions) on Wiley Online Library for rules of use; OA articles are governed by the applicable Creative Commons License

Results and discussion

Capacity

Bed height and mobile-phase velocity both affect the dynamic capacity; together bed height and flow rate determine the residence time. The inverse of residence time is flow rate in $CV \cdot h^{-1}$, calculated as the superficial mobile-phase velocity (measured in $cm \cdot h^{-1}$) divided by the bed height (measured in cm). A flow-rate measurement in $CV \cdot h^{-1}$ is independent of scale and is also independent of the aspect ratio of the column. Dynamic capacity was related logarithmically to the flow rate in $CV \cdot h^{-1}$ (Figure 1). At 500 $cm \cdot h^{-1}$ on a 10-cm-long column (50 $CV \cdot h^{-1}$) there is a significant difference in dynamic capacity for the five sorbents (Table 1). Poros LP sorbent had about 15% less capacity than Poros 50, as would be expected from the larger average particle size of the Poros LP.

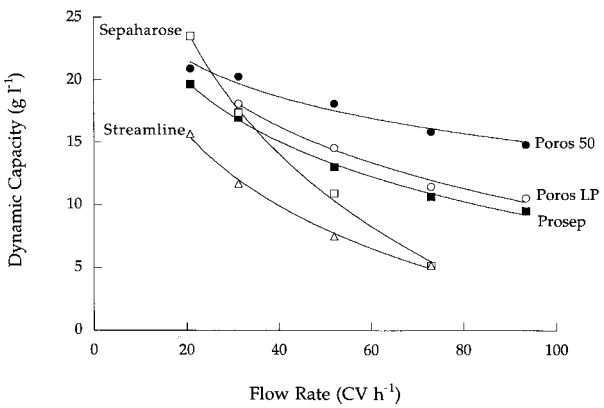

Figure 1 The effect of flow rate on dynamic capacity for five Protein A affinity-chromatography sorbents

Dynamic capacity (g of antibody/l of CV) was measured on 10-cm-long columns at 1% breakthrough determined by the online assay. □, Sepharose [$y = 66.9\text{-}33.0 \cdot \log(x)$, $R^2 = 0.997$]; ●, Poros 50 [$y = 34.3 - 9.77 \cdot \log(x)$, $R^2 = 0.963$]; ○, Poros LP [$y = 42.8 - 16.5 \cdot \log(x)$, $R^2 = 0.988$]; ■, Prosep [$y = 40.8 - 16.0 \cdot \log(x)$, $R^2 = 0.996$]; △, Streamline [$y = 40.8 - 19.2 \cdot \log(x)$, $R^2 = 0.995$].

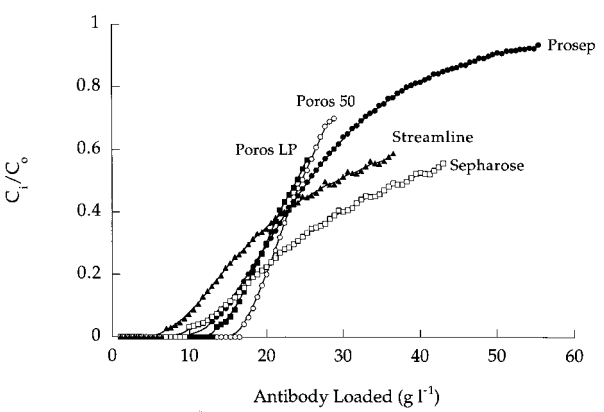

Figure 2 Partial breakthrough curves for five Protein A affinity-chromatography sorbents

Chromatography was performed with a 10-cm-long column and 500 $cm \cdot h^{-1}$ flow rate (50 $CV \cdot h^{-1}$). Breakthrough was measured by online assay. Antibody loaded (g of antibody/l of CV) means antibody loaded into the column, $F_1 \cdot C_o \cdot t/V_c$ (where F is volumetric flow rate for load and t is time). ●, Prosep; □, Sepharose; ■, Poros LP; ○, Poros 50; ▲, Streamline.

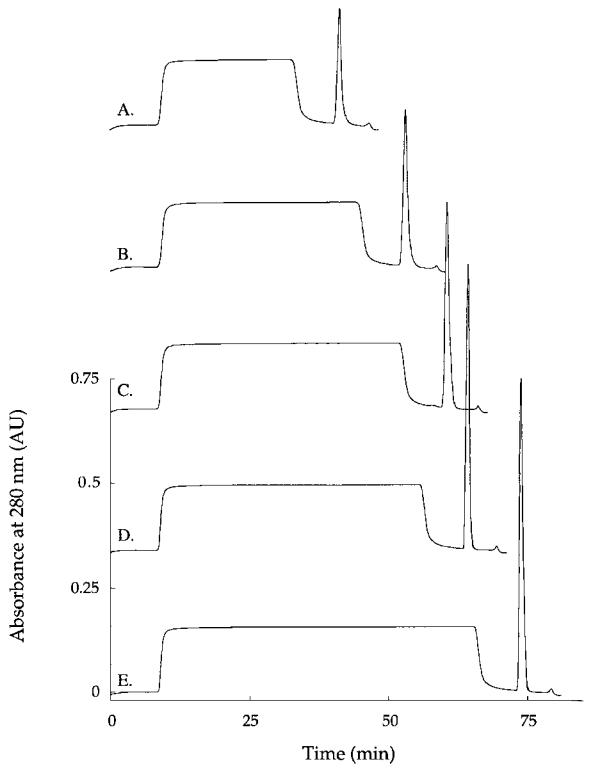

Figure 3 Chromatograms for five Protein A affinity-chromatography sorbents

Load was ended at 1% breakthrough, measured by online assay; 1 × 10-cm columns, 500 $cm \cdot h^{-1}$ flow rate. A, Streamline; B, Sepharose; C, Prosep; D, Poros LP; E, Poros 50.

For breakthrough curves that are symmetrical around $C_i/C_o = 0.5$ (where C_i is the antibody concentration in the column effluent), the saturation (or total) capacity is equal to the antibody loaded into the column at $C_i/C_o = 0.5$. We generated partial breakthrough curves for the five sorbents, loading clarified cell culture fluid and measuring breakthrough with the online assay (Figure 2). Whereas not all breakthrough curves appear to be symmetrical because of the relatively high flow rate used (50 $CV \cdot h^{-1}$), they can be used to estimate saturation capacity (Table 1). In this study, Sepharose had the highest saturation capacity, and Poros LP had slightly less saturation capacity than Poros 50.

Chromatograms and yield

All chromatograms show a good shape for breakthrough fronts and sharp elution peaks (Figure 3). Peaks eluted sharply with 0.1 M acetic acid, with no precipitation. Yield

© 1999 Portland Press Ltd

14708744, 1999, 2, Downloaded from https://iubmb.onlinelibrary.wiley.com/doi/10.1111/j.1470-8744.1999.tb00902.x by Test, Wiley Online Library on [16/10/2023]. See the Terms and Conditions (https://onlinelibrary.wiley.com/terms-and-conditions) on Wiley Online Library for rules of use; OA articles are governed by the applicable Creative Commons License

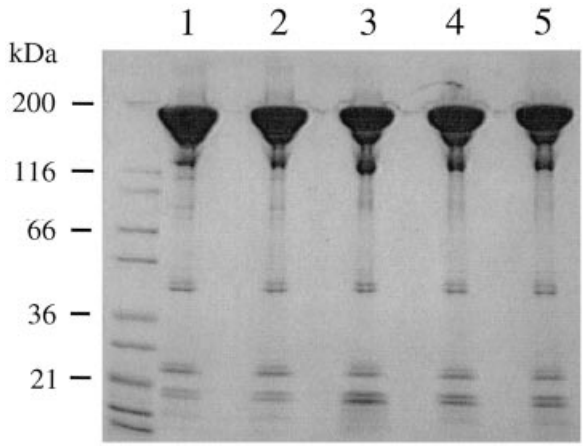

Figure 4 SDS/PAGE of antibody purified on five Protein A affinity-chromatography sorbents

The runs used 10-cm-long columns and 500 cm·h^{-1} flow rates (50 CV·h^{-1}) loaded to dynamic capacity determined at 1% breakthrough. Lane 1, Poros 50; lane 2, Poros LP; lane 3, Prosep; lane 4, Sepharose Fast Flow; lane 5, Streamline.

for all of these sorbents was at least 100% (Table 1), indicating that all bound antibody was eluted with 0.1 M acetic acid, and that the online assay could reliably stop loading at 1% breakthrough. The antibody concentration in the pool varied (Table 1), primarily because of the varying load on the column. However, another contribution may have been the slightly wider elution peaks observed for Sepharose and Streamline (Figure 3), which would be expected for these large-particle-size sorbents at these relatively high flow rates.

Purity

The purity of antibody purified on each sorbent was measured by SDS/PAGE, host-cell proteins and DNA. In this study, we compared columns each loaded to their dynamic capacity rather than each loaded to the same capacity.

SDS/PAGE (Figure 4) shows equivalent purity, with no new protein bands. A quantitative measurement by ELISA of the amount of host-cell proteins (Table 1) revealed small differences in the antibody purity, with values from 2.5 to 6.1 mg·g^{-1}(mg of host-cell proteins/g of antibody). The amount of host-cell proteins in the load was approx. 950 mg·g^{-1}, so these represent a range from 380- to 150-fold clearance. The Poros sorbents may have the least non-specific binding, since both Poros 50 and Poros LP had low values for host-cell proteins. However, even the lowest clearance (for Streamline) this represents a 99.36% removal of host-cell proteins. The lowest clearance for packed-bed sorbents (Sepharose) was a 99.48% clearance. All of the values for host-cell proteins represent significant antibody purification, and these sorbents would most probably be interchangeable for host-cell-protein clearance. Complete antibody recovery processes often contain both anion-exchange and cation-exchange columns downstream of the Protein A step, which together provide significant clearance of host-cell proteins, and the small differences observed here would most probably disappear as the product moves downstream.

We did not optimize the methods for removal of host-cell proteins, and an intermediate wash may have increased host-cell-protein removal. For example, controlled-pore glass sorbents are sometimes washed with tetramethyl-ammonium chloride after loading to reduce the level of host-cell proteins, which may be non-specifically bound to the chromatography medium. Washing the Prosep with 3 CV of 25 mM Tris/25 mM NaCl/5 mM EDTA/0.5 M tetramethyl-ammonium chloride (pH 7.0) slightly reduced the level of host-cell proteins from 3.7±0.2 to 3.0±0.4 mg·g^{-1}.

All sorbents provided significant DNA clearance (Table 1). The amount of DNA in the clarified cell-culture fluid was approx. 9700 ng·mg^{-1}. Thus the amount of DNA in the purified antibody pools represented from 98.99% DNA removal (100-fold) for Streamline to 99.7% (330-fold) for Sepharose. Sepharose may have the lowest level of non-specific DNA binding. The lowest level of DNA clearance for the packed-bed sorbents was 99.51% (200-fold) for Poros LP. All of these DNA values were low, and downstream recovery steps often provide significant DNA clearance, so the sorbents would probably be interchangeable for DNA clearance. We did not optimize the wash for DNA clearance, and additional DNA clearance could possibly have been gained by including a longer wash between the load and elution, or by including an intermediate wash.

The amount of Protein A varied from 3.1 ng·mg^{-1} for Prosep to 7.7 ng·mg^{-1} for Poros LP. All of these levels were very low, and would most probably have been cleared to less than detectable levels downstream of the Protein A step. The sorbents are most probably interchangeable for Protein A leaching.

Production rate

In a simple consideration of production rate, the four packed-bed sorbents in the same column dimensions would have approximately the same production rate at about 25 CV·h^{-1}. This is because the dynamic capacity would be about the same, with the caveat that some column lengths would not be feasible because of back-pressure limitations (primarily for Poros 50) or flow-rate limitations (primarily for Sepharose). For example, at 25 CV·h^{-1} on a 15-cm-long column at 375 cm·h^{-1}, all the sorbents would have approximately the same capacity, and the media would be essentially interchangeable since they all provide approximately equivalent purification. As the flow rate increased, the differences in production rate would become apparent as the dynamic capacities became different as less antibody was loaded.

© 1999 Portland Press Ltd

14708744, 1999, 2, Downloaded from https://iubmb.onlinelibrary.wiley.com/doi/10.1111/j.1470-8744.1999.tb00902.x by Test, Wiley Online Library on [16/10/2023]. See the Terms and Conditions (https://onlinelibrary.wiley.com/terms-and-conditions) on Wiley Online Library for rules of use; OA articles are governed by the applicable Creative Commons License

A more detailed consideration of production rate could introduce several complexities. The production rate would be maximized when the flow rate used for the elution, equilibration and wash was run at the highest possible value. Limits on the flow rate would include media compressibility (particularly for Sepharose), process equipment and pressure drop. Because the permeabilities of the sorbents are different, the pressure drop across a packed bed varies (Table 1). This means that at a given column length in a packed bed, each sorbent will have a different maximum flow rate. Because both the pressure drop and the dynamic capacity will vary with column length and flow rate, the comparison and optimization of production rate for each sorbent is complicated. Here we use the simple production-rate equations (eqns. 2 and 3) to visualize the effect of flow rate and column length on production rate. We did not include Streamline in this study, since the production rate for expanded-bed applications depends on several factors that do not apply to packed beds (for example whether the column is eluted in packed- or expanded-bed mode).

The production-rate equations (eqns. 2 and 3) were used to determine the effect of flow rate and column length on production rate. In eqn. (2), R_{pa} depends on five factors: the dynamic capacity (Q_d), the antibody concentration in the load (C_o), the number of CVs for elution/equilibration/wash (N), the load flow rate (U_l) and the elution/equilibration/wash flow rate (U_e). Eqn. (3) adds L_c for R_{pv}. By substituting functions for Q_d and U_e, eqns. (2) and (3) can be reduced to depend only on the variables of the load flow rate (U_l) and the column length (L_c), and the constants C_o and N.

To use the production-rate equations, we made several assumptions and imposed several constraints. Since Protein A affinity-chromatography medium is expensive, the process is sometimes optimized to maximize dynamic capacity to use as much of the Protein A sorbent as possible, but we assumed that the dynamic capacity could be any value in the range studied in Figure 1 (we chose production rate rather than dynamic capacity for optimization). Although increasing load beyond the dynamic capacity can increase production rate [22], Protein A affinity chromatography of recombinant antibodies is most often run at maximum yield to prevent loss of expensive product, and we assumed that the process would be run at the dynamic capacity. We assumed that the minimum column length was 10 cm, since a shorter column would be difficult to pack and run reliably in a process application, and we assumed that the maximum superficial mobile-phase velocity was 750 cm·h^{-1} for Sepharose (above which the medium can compress) and 1500 cm·h^{-1} for the other sorbents (because flow rates greater than 1500 cm·h^{-1} may be impractical for process applications). We assumed that the maximum pressure at the column inlet was 2×10^5 Pa (valid for many process columns), and that the contribution of the system to the inlet pressure (in Pa) was equal to $70 \cdot U$. To express U_e as a function of L_c, U_e is run at the maximum inlet pressure, a function of L_c and U_e, with an upper limit of 1500 cm·h^{-1}. We used $C_o = 0.35$ g·l^{-1} and $N = 16$. We used only values of flow rate where we measured dynamic capacity, 20–95 CV·h^{-1}. We used Q_d as a function of flow rate in CV·h^{-1} (calculated as U_l/L_c), given by the logarithmic fits in Figure 1.

With these assumptions and constraints the production-rate equations are dependent only on the variables L_c and U_l. We used eqns. (2) and (3) to construct a plot to visualize the effect of flow rate and column length on production rate and also to find the optimal flow rate and column length for maximum production rate. Production rate has a composite dependence on L_c and U_l (Figure 5).

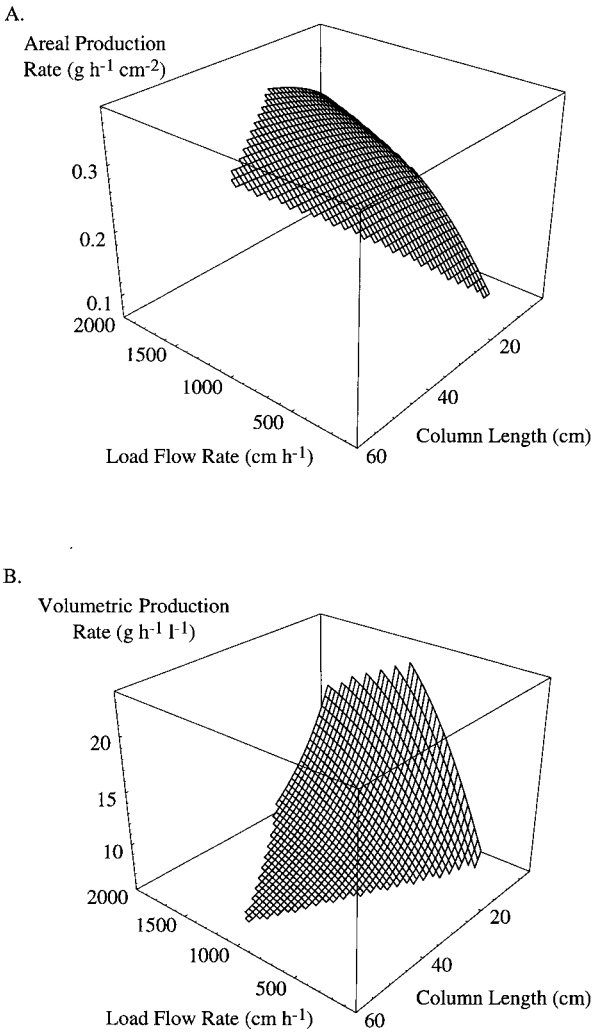

Figure 5 The effect of the load flow rate and column length on the production rate for Prosep media

Production rate was calculated using eqns. (2) and (3) and the assumptions and constraints described in the text. (**A**) Areal production rate (g of antibody/h per cm^2 of column cross-sectional area), calculated using eqn. (2). (**B**) Volumetric production rate (g of antibody/h per l of CV), calculated using eqn. (3).

© 1999 Portland Press Ltd

14708744, 1999, 2, Downloaded from https://iubmb.onlinelibrary.wiley.com/doi/10.1111/j.1470-8744.1999.tb00902.x by Test, Wiley Online Library on [16/10/2023]. See the Terms and Conditions (https://onlinelibrary.wiley.com/terms-and-conditions) on Wiley Online Library for rules of use; OA articles are governed by the applicable Creative Commons License

14708744, 1999, 2, Downloaded from https://iubmb.onlinelibrary.wiley.com/doi/10.1111/j.1470-8744.1999.tb00902.x by Test, Wiley Online Library on [16/10/2023]. See the Terms and Conditions (https://onlinelibrary.wiley.com/terms-and-conditions) on Wiley Online Library for rules of use; OA articles are governed by the applicable Creative Commons License

Figure 5 shows the operating region bounded by constraints on the flow rate, column length and inlet pressure. When optimizing for areal production rate (Figure 5A), for most values of column length the production rate increases as the load flow rate increases, even though dynamic capacity is decreasing. This is because, although more cycles would be required to process a given amount of antibody, each cycle is run very quickly, and the overall production rate increases. The increased number of cycles needed due to the lower dynamic capacity is offset by the higher throughput of each cycle. For Prosep media (Figure 5A), the optimal areal production rate (Table 1) was at $U_e = 1490\ cm \cdot h^{-1}$, $U_l = 1500\ cm \cdot h^{-1}$ and $L_c = 34.3$ cm. The volumetric production rate has a different dependence on load flow rate and column length (Figure 5B), although it is still true that for most values of column length, the production rate increases as the load flow rate increases. For Prosep media (Figure 5B), the optimal volumetric production rate (Table 1) is at $U_e = 1020\ cm \cdot h^{-1}$, $U_l = 1500\ cm \cdot h^{-1}$ and $L_c = 11.1$ cm. By constructing similar plots for the other sorbents, the optimal production rates may be found for the other sorbents (Table 1).

An interesting consequence of production-rate optimization can be seen in the difference between Poros 50 and Poros LP. For both areal and volumetric production rate, Poros LP had higher values than Poros 50. This demonstrates that, although Poros 50 had a higher dynamic capacity at the flow rates studied (Figure 1), the fact that Poros LP had a lower pressure drop (higher permeability) gives it a higher production rate. This observation may impact the design of affinity sorbents, where a trade off between particle-size distribution, dynamic capacity and production rate can be made. A small difference in the particle-size distribution can have a large impact on process design, and there may be an optimal particle-size distribution for maximum production rate.

For areal production rate, Prosep has the highest value (Table 1), primarily because of its low pressure drop that extends its operating range. Both Prosep and Poros LP have the highest values of volumetric production rate. Because the dynamic capacity of Sepharose increases sharply at low flow rates (Figure 1), extending the operating region to flow rates below $20\ CV \cdot h^{-1}$ may reveal areas of higher production rate, particularly if the dynamic capacity follows a power function rather than a logarithmic function at lower flow rates. All of these sorbents provide production rates that would be compatible for process applications.

Other considerations

One important factor for process applications that was not addressed in this study is the effect of column reuse. Because Protein A affinity-chromatography media are expensive, rather than processing a batch of antibody in a single cycle, the batch is often purified over many cycles of a smaller column, and the ability of a sorbent to withstand extreme reuse could be a significant performance factor. The recovery process for monoclonal antibodies must provide virus clearance. Often, Protein A affinity chromatography can provide some virus clearance, but we did not measure the clearance of viruses for any of the sorbents. Finally, there are many other commercial sorbents available, with different base media and Protein A-coupling chemistries.

Acknowledgments

For their generous contributions, we thank Matt Fields, Chris Schuetz and Genentech's Protein A action group.

References

1 Thommes, J., Bader, A., Halfar, M., Karau, A. and Kula, M.-R. (1996) J. Chromatogr. A **752**, 111–122
2 Chase, H. A. and Draeger, N. M. (1992) J. Chromatogr. **597**, 129–145
3 Fuglistaller, P. (1989) J. Immunol. Methods **124**, 171–177
4 Hjelm, H., Hjelm, K. and Sjoquist, J. (1972) FEBS Lett. **28**, 73–76
5 Kamiya, Y., Majima, T., Sohma, Y., Katoh, S. and Sada, E. (1990) J. Ferment. Bioeng. **69**, 298–301
6 Schuler, G. and Reinacher, M. (1991) J. Chromatogr. **587**, 61–70
7 Tu, Y. Y., Primus, F. J. and Goldenberg, D. M. (1988) **109**, 43–47
8 Van Sommeren, A. P. G., Machielsen, P. A. G. M. and Gribnau, T. C. J. (1992) Prep. Biochem. **22**, 135–149
9 Ey, P. L., Prowse, S. J. and Jenkin, C. R. (1978) Immunochemistry **15**, 429–436
10 Carter, P., Presta, L., Gorman, C. M., Ridgway, J. B. B., Henner, D., Wong, W. L. T., Rowland, A. M., Kotts, C., Carver, M. E. and Shepard, H. M. (1992) Proc. Natl. Acad. Sci. U.S.A. **89**, 4285–4289
11 Bodey, B., Kaiser, H. E. and Goldfarb, R. H. (1996) Anticancer Res. **16**, 517–532
12 Anderson, D. R., Grillo-Lopez, A., Varns, C., Chambers, K. S. and Hanna, N. (1996) Biochem. Soc. Trans. **25**, 705–708
13 Longo, D. L. (1996) Curr. Opin. Oncol. **8**, 353–359
14 Baselga, J., Tripathy, D., Mendelsohn, J., Baughman, S., Benz, C. C., Dantis, L., Sklarin, N. T., Seidman, A. D., Hudis, C. A., Moore, J. et al. (1996) J. Clin. Oncol. **14**, 737–744
15 Surolia, A., Pain, D. and Khan, M. I. (1982) Trends. Biochem. Sci. **7**, 74–76
16 Reis, K. J., Boyle, M. D. P. and Ayoub, E. M. (1984) J. Clin. Lab. Immunol. **13**, 75–80
17 Lindmark, R., Thoren-Tolling, K. and Sjoquist, J. (1983) J. Immunol. Methods **62**, 1–13

© 1999 Portland Press Ltd

18 Katoh, S., Kambayashi, T., Deguchi, R. and Yoshida, F. (1978) Biotechnol. Bioeng. **20**, 267–280
19 Kang, K. A. and Ryu, D. D. Y. (1991) Biotechnol. Progr. **7**, 205–212
20 Mao, Q. M., Prince, I. G. and Hearn, M. T. W. (1995) J. Chromatogr. A **691**, 273–283
21 Jandera, P., Komers, D. and Guichon, G. (1997) J. Chromatogr. A **760**, 25–39
22 Mao, Q. M., Prince, I. G. and Hearn, M. T. W. (1993) J. Chromatogr. **646**, 81–89
23 Felinger, A. and Guiochon, G. (1992) J. Chromatogr. **591**, 31–45
24 Katoh, S. (1987) Trends Biotechnol. **5**, 328–331
25 Horstmann, B. J. and Chase, H. A. (1989) Chem. Eng. Res. Des. **67**, 243–254
26 Yamamoto, S. and Sano, Y. (1992) J. Chromatogr. **597**, 173–179
27 van Reis, R., Leonard, L. C., Hsu, C. C. and Builder, S. E. (1991) Biotechnol. Bioeng. **38**, 413–422
28 Afeyan, N. B., Gordon, N. F., Mazaroff, I., Varady, L., Fulton, S. P., Yang, Y. B. and Regnier, F. E. (1990) J. Chromatogr. **519**, 1–29
29 McCoy, M., Kalghatgi, K., Regnier, F. E. and Afeyan, N. (1996) J. Chromatogr. A **743**, 221–229
30 Whitney, D., McCoy, M., Gordon, N. and Afeyan, N. (1998) J. Chromatogr. A **807**, 165–184
31 Varady, L., Mu, N., Yang, Y. B., Cook, S. E., Afeyan, N. and Regnier, F. E. (1993) J. Chromatogr. **631**, 107–114
32 Fahrner, R. L. and Blank, G. S. (1999) Biotechnol. Appl. Biochem. **29**, 109–112
33 Chen, A. B. (1996) J. Biotechnol. Healthcare **3**, 70–80

Received 4 May 1999; accepted 2 June 1999

© 1999 Portland Press Ltd

14708744, 1999, 2, Downloaded from https://iubmb.onlinelibrary.wiley.com/doi/10.1111/j.1470-8744.1999.tb00902.x by Test, Wiley Online Library on [16/10/2023]. See the Terms and Conditions (https://onlinelibrary.wiley.com/terms-and-conditions) on Wiley Online Library for rules of use; OA articles are governed by the applicable Creative Commons License